Cellular Physiology and Biochemistry

Cell Physiol Biochem 2016;39:278-293
DOI: 10.1159/000445623
Published online: June 24, 2016
Accepted: May 31, 2016

1421-9778/16/0391-0278$39.50/0
www.karger.com/cpb

Original Paper

Quercetin Stimulates Insulin Secretion and Reduces the Viability of Rat INS-1 Beta-Cells

Michael Kittl[a] Marlena Beyreis[a] Munkhtuya Tumurkhuu[a,b] Johannes Fürst[c] Katharina Helm[a] Anna Pitschmann[d] Martin Gaisberger[a,e,f] Sabine Glasl[d] Markus Ritter[a,e,f] Martin Jakab[a]

[a]Institute of Physiology and Pathophysiology, Paracelsus Medical University, Salzburg, Austria; [b]School of Pharmacy and Bio-Medicine, Mongolian National University of Medical Sciences, Ulaanbaatar, Mongolia; [c]Department of Physiology and Medical Physics, Division of Physiology, Medical University of Innsbruck, Innsbruck, Austria; [d]Department of Pharmacognosy, University of Vienna, Vienna, Austria; [e]Department for Radon Therapy Research, Ludwig Boltzmann Cluster for Arthritis and Rehabilitation, Salzburg, Austria; [f]Gastein Research Institute, Paracelsus Medical University, Salzburg, Austria

Key Words
Flavonoid • Quercetin • Rutin • Insulin • INS-1 • Beta-cells • Apoptosis • Viability • Current • Calcium • Potassium • K_{ATP} • K_{ir} 6.2 • ATP-sensitive

Abstract
Background/Aims: Previously we described insulinotropic effects of *Leonurus sibiricus* L. plant extracts used for diabetes mellitus treatment in Traditional Mongolian Medicine. The flavonoid quercetin and its glycoside rutin, which exert anti-diabetic properties *in vivo* by interfering with insulin signaling in peripheral target tissues, are constituents of these extracts. This study was performed to better understand short- and long-term effects of quercetin and rutin on beta-cells. ***Methods:*** Cell viability, apoptosis, phospho-protein abundance and insulin release were determined using resazurin, annexin-V binding assays, Western blot and ELISA, respectively. Membrane potentials (V_{mem}), whole-cell Ca^{2+} (ICa)- and ATP-sensitive K^+ (IK_{ATP}) currents were measured by patch clamp. Intracellular Ca^{2+} (Ca_i) levels were measured by time-lapse imaging using the ratiometric Ca^{2+} indicator Fura-2. ***Results:*** Rutin, quercetin and the phosphoinositide-3-kinase (PI3K) inhibitor LY294002 caused a dose-dependent reduction in cell viability with IC_{50} values of ~75 µM, ~25 µM and ~3.5 µM, respectively. Quercetin (50 µM) significantly increased the percentage of Annexin-V+ cells within 48 hrs. The mean cell volume (MCV) of quercetin-treated cells was significantly lower. Within 2 hrs, quercetin significantly decreased basal- and insulin-stimulated Akt(T308) phosphorylation and increased Erk1/2 phosphorylation, without affecting P-Akt(S473) abundance. Basal- and glucose-stimulated insulin release were significantly stimulated by quercetin. Quercetin significantly depolarized V_{mem} by ~25 mV which was prevented by the K_{ATP}-channel opener diazoxide, but not by the

M. Kittl and M. Beyreis contributed equally to this work.

Martin Jakab

Paracelsus Medical University, Institute of Physiology and Pathophysiology, Strubergasse 22, 5020 Salzburg, (Austria)
Tel. +43-662-242080504, E-Mail martin.jakab@pmu.ac.at

L-type ICa inhibitor nifedipine. Quercetin significantly stimulated ICa and caused a 50% inhibition of IK_{ATP} . The effects on V_{mem}, ICa and IK_{ATP} rapidly reached peak values and then gradually diminished to control values within ~1 minute. With a similar time-response quercetin induced an elevation in Ca_i which was completely abolished in the absence of Ca^{2+} in the bath solution. Rutin (50 µM) did not significantly alter the percentage of Annexin-V+ cells, MCV, Akt or Erk1/2 phosphorylation, insulin secretion, or the electrophysiological behavior of INS-1 cells. ***Conclusion:*** We conclude that quercetin acutely stimulates insulin release, presumably by transient K_{ATP} channel inhibition and ICa stimulation. Long term application of quercetin inhibits cell proliferation and induces apoptosis, most likely by inhibition of PI3K/Akt signaling.

Introduction

In a previous study we described the insulinotropic effects of *Leonurus sibiricus* L. (LS) plant extracts used in Traditional Mongolian Medicine (TMM) for the treatment of diabetes mellitus (DM) and DM-related symptoms [1]. We have demonstrated that insulin release from INS-1E cells was significantly increased in presence of aqueous as well as methanolic LS extracts. Acute application of water extract resulted in a persisting depolarization of the cell membrane potential (V_{mem}) paralleled by an initial increase and subsequent silencing of action potential frequency, by K_{ATP} channel inhibition and an increase in intracellular calcium (Ca_i). Furthermore, all LS extracts stimulated INS-1E cell proliferation. The present study was performed to identify LS extract compounds accounting for the observed effects on beta-cell viability, insulin release and electrophysiological behavior. We focused on the flavonoid quercetin and its glycoside rutin, two phytochemicals which could be identified as constituents of LS extracts by HPLC analyses [1, 2] and which are known to exert comparable effects in different cell systems.

Quercetin is a naturally occurring flavonoid commonly found in plants. It is the aglycone of a number of flavonoid glycosides including rutin [3]. In the gut quercetin is formed through hydrolysis of rutin by intestinal microorganisms [4]. The pharmacological actions of rutin and quercetin include inhibition of lipopolysaccharide-induced nitric oxide production, antioxidant, anti-hyperglycemic, anti-inflammatory, cytoprotective, hepatoprotective and chemopreventive activities [5-12]. In several cell types including pancreatic beta-cells it suppresses NF-κβ, decreases pro-inflammatory cytokines and suppresses the production of oxidized LDL and TNF-α [13-16]. Both rutin and quercetin show insulinotropic properties *in vivo* and *in vitro*, have beneficial effects in metabolic syndrome and exert anti-diabetic properties. Studies in animals and humans have suggested its potential in the treatment of metabolic syndrome and diabetes [13, 17-33].

Rutin and quercetin act on cellular signaling mechanisms on many levels and affect e.g. glucose transport, metabolism, cell proliferation and survival. In rat skeletal muscle rutin stimulates Ca^{2+} uptake from the extracellular space through voltage-gated Ca^{2+} channels and glucose uptake is increased as a consequence of calcium-calmodulin-dependent protein kinase II (CaMKII)-stimulated glucose transporter (GLUT)-4 translocation to the plasma membrane [34]. Rutin has further been shown to enhance insulin-dependent GLUT-4 translocation by insulin-receptor (IR) tyrosin kinase activation [35]. Quercetin and its metabolite quercetin-3-O-methylglucose were shown to protect the umbilical vein endothelium against oxidative stress-induced inflammation and insulin resistance. Both compounds facilitated phosphoinositide-3-kinase (PI3K) signaling by positive regulation of serine/tyrosine phosphorylation of IR substrate (IRS)-1 and restoration of downstream Akt/eNOS activation [36]. In INS-1 insulinoma cells quercetin potentiates glucose- and glibenclamide-induced insulin release and Erk1/2 phosphorylation and protects the cells against H_2O_2-induced oxidative damage [19]. In the same cells as well as in isolated rat pancreatic islets quercetin has been found to enhance insulin secretion by direct activation of L-type Ca^{2+} channels [17]. In INS-1E insulinoma cells quercetin enhances glucose-induced

insulin secretion under hyperglycemic and glycotoxic conditions and it modulates gene expression profiles – including GLUT-2, glucokinase, insulin receptor substrate (IRS-1), Akt1/2, Bcl2 and Bax among others [18] – to improve beta-cell survival and function during glucotoxicity. Quercetin affects cell proliferation and cell death. Recently it was shown that in mouse MC3T3-G2/PA6 cells differentiated into mature adipose cells quercetin inhibits insulin-stimulated glucose uptake and IR-beta subunit phosphorylation, while rutin was without effect. Moreover, quercetin appears to inhibit insulin-stimulated activation of Akt and suppresses insulin-dependent GLUT-4 translocation to the plasma membrane [37]. In MDA-MB-231 breast cancer cells quercetin suppresses insulin-induced IR dimerization by interfering with ligand-receptor interactions, which reduces the phosphorylation of IR and Akt. This further inhibits insulin stimulated glucose uptake due to impaired translocation of GLUT-4 to the cell membrane leading to impaired cancer cell proliferation [38]. By inhibiting the PI3K/Akt pathway quercetin also inhibits proliferation of HeLa cells and breast carcinoma cell lines and induces apoptosis in promyelocytic HL-60 cells [39-41]. In HepG2 hepatocellular carcinoma cells quercetin was found to mediate autophagy by release of Ca^{2+} from intracellular stores [42] and to enhance apoptosis by induction of a positive feedback loop consisting of p53, miR-34a miRNA and SIRT1 [43].

The present study was performed to investigate short and long-term effects of quercetin and rutin on beta-cells [1, 2]. While most studies which describe insulinotropic influences of flavonoids on beta-cells focus on short term effects, data on chronic exposure are lacking. We designed this study to investigate both long- and short term effects on insulin secreting cells using rat INS-1 cells – a beta-cell model well described with respect to proliferation, pro- and anti-apoptotic signal transduction pathways, insulin release and electrophysiological behavior [19, 44-49]. Cell viability, apoptosis, phospho(P)-Akt and P-Erk1/2 protein abundance and insulin release were determined and cell membrane potentials (V_{mem}), whole-cell Ca^{2+} (ICa)- and ATP-sensitive K^+ (IK_{ATP}) currents and intracellular Ca^{2+} (Ca_i) concentrations were measured.

Materials and Methods

Chemicals and reagents

All salts and chemicals used for the preparation of experimental solutions and cell culture media were p.a. grade. Tolbutamide, LY294002 and porcine insulin were purchased from Sigma-Aldrich. Rutin (Quercetin-3-rutoside) and quercetin were from Carl Roth. Stock solutions of rutin, quercetin and LY294002 (50 or 100, and 10 mM, respectively) were prepared in dimethyl sulfoxide (DMSO). Tolbutamide was dissolved in ethanol at a stock concentration of 100 mM. Resazurin was obtained from Sigma Aldrich and dissolved in phosphate buffered saline (PBS) to give a 2.5 mM stock solution. Stocks were stored in aliquots at -20°C until use.

Cell culture

For cell viability measurements, Western blot experiments, flow cytometry and electrophysiological recordings, INS-1 cells [48] were grown in RPMI 1640 medium containing 11.1 mM D-glucose, 1 mM sodium pyruvate, 50 µM β-mercaptoethanol, 2 mM glutamine, 10 mM HEPES, 10% fetal calf serum (FCS), 100 U/mL penicillin, 100 µg/mL streptomycin, and 250 ng/mL amphotericin B at 37°C, humidified 5% CO_2 and 95% air (standard conditions). Subcultures were established once a week by trypsin/EDTA treatment. Cells within passages 100 and 120 were used for the experiments.

Cell viability

For cell viability measurements INS-1 cells were seeded in black, clear bottom, tissue culture treated 96-well microplates at a density of 12,500 cells/well. After over-night incubation under standard conditions cells were either left untreated, incubated in culture medium containing rutin or quercetin (1.5, 3.1, 6.25, 12.5, 25, 50 and 100 µM), LY294002 (1, 10 or 100 µM), or 0.1% (v/v) DMSO (solvent control) for further 48 hrs. Insulin (10 µM) was added to the culture medium as indicated. Triton X-100 (1% v/v) causing maximum

cell damage was used as positive control. Experimental conditions were run in 5–6 replicates per plate. For quantification of cell viability a resazurin (alamar blue) assay was used [50]. This assay is a fluorescence-based assay to determine the number of viable, metabolically active cells, given that only viable cells are able to metabolize resazurin to the fluorescent resorufin. The reduction of resazurin to resorufin is irreversible and fluorescence intensity is proportional to the amount of viable cells. Resazurin was used at a final concentration of 0.5 mM. Fluorescence measurements were performed on a Zenyth 3100 multimode reader (Anthos Labtec Instruments GmbH, Austria). Excitation and emission wavelength were 535 and 595 nm, respectively. For background subtraction background fluorescence was determined for each experimental treatment from blank, cell-free wells containing incubation medium with drugs only. Data are presented as relative fluorescence units (RFU). As the reduction of resazurin depends on cell metabolism, changes in fluorescence might be caused by effects on the cells' metabolic state rather than the absolute number of viable cells. To validate the resazurin assay we therefore performed a parallel series of experiments based on live-cell protease activity assessment using a fluorogenic, cell-permeant, peptide substrate (CellTiter Fluor™ cell viability assay; Promega). Intracellular cleavage of the substrate by a conserved and constitutively active protease generates a fluorescent signal proportional to the number of living cells. The results obtained with this assay were identical to those of the resazurin assay (n = 3; data not shown).

Flow cytometry

For assessment of phosphatidylserine exposure at the cell surface by Annexin-V binding and cell membrane integrity by 7-actinomycin D (7-AAD) staining, cells were seeded in 30 mm diameter petri dishes at a density of 600,000 cells/dish. Following over night culture under standard conditions, cells were either left untreated, or incubated with 50 µM rutin, 50 µM quercetin, or 0.1% (v/v) DMSO (solvent control) in absence or presence of 10 µM insulin for 48 hrs. Thereafter cells were harvested by trypsin/EDTA treatment, washed twice in PBS and resuspended in the binding buffer to a concentration of 1×10^6 cells/ml. 100 µl of the respective cell suspensions were subjected to staining for 15 minutes in the dark with FITC (fluorescein isothiocyanate)-conjugated Annexin-V and 7-AAD (BioLegend, Inc., USA) according to the manufacturer's protocol. After addition of 400 µl binding buffer to each sample, cells were analyzed by flow cytometry. Fluorescence emissions of FITC-Annexin-V on FL-1 (525 nm band pass filter) and 7-AAD on FL-3 (670 nm long pass filter) were measured upon excitation with a 488-nm argon laser using a Cell Lab Quanta™ SC flow cytometer (Beckman-Coulter). Unstained and single-stained samples were used for setting the electronic volume (EV) gain, FL-1 and FL-3 PMT-voltages and for compensation of FITC-spill over into the 7-AAD channel. Debris (particles diameter <7 µm) and cell aggregates (>20 µm) were excluded from analysis. 30,000–50,000 single cells (diameter 7–20 µm) were analyzed in each sample. Parameter dividers were set to segregate Annexin-V– and Annexin-V+ cells. Cell diameter/volume was directly measured with the Cell Lab Quanta™ employing the Coulter principle for volume assessment, which is based on measuring changes in electrical resistance produced by nonconductive particles suspended in an electrolyte solution. The electronic volume channel was calibrated using 10 µm Flow-Check fluorospheres (Beckman-Coulter) by positioning this size bead in channel 200 on the volume scale. The mean cell volume (MCV) is given in femtoliters (fl).

Western blot

For analysis of phospho-protein abundance, cells were seeded in 30 mm petri dishes at a density of 10^6 cells/dish and grown for 48 hrs under standard conditions to 70–80% confluence. Subconfluent cells were incubated for 2 hrs in culture medium containing 50 µM rutin, 50 µM quercetin, 0.1% (v/v) DMSO (solvent control) in absence or presence of 10 µM insulin, or left untreated. After the incubation period culture media were aspirated and cells were washed with ice cold PBS. Cells were scraped off with lysis buffer composed of 20 mM Tris-HCl (pH 7.5), 150 mM NaCl, 1 mM Na_2EDTA, 1 mM EGTA, 1% Triton X-100, 2.5 mM sodium pyrophosphate, 1 mM β-glycerophosphate, 1 mM Na_3VO_4, 1 µg/ml leupeptin and 1 mM phenylmethanesulfonyl fluoride (PMSF). Cell lysates were sonicated (5×1 second) and centrifuged at 13,000×g for 10 minutes. Samples were mixed with 2× sample buffer containing 125 mM TRIS-HCl, 4% (w/v) SDS, 0.7% (v/v) β-mercaptoethanol, 20% (v/v) glycerol and 0.004% (w/v) bromphenol blue, and 25 µl/sample were separated by SDS-PAGE on 4–20% Mini-PROTEAN® TGX™ gels (Bio-Rad, Germany). Proteins were transferred onto 0.2 µm nitrocellulose membranes using a Bio-Rad Trans-Blot® Turbo™ system. Membranes were incubated over night at 4°C with rabbit monoclonal antibodies against total Akt

(pan), phospho-Akt (Thr308), phospho-Akt (Ser473), total Erk1/2 (p44/42 MAPK), or phospho-Erk1/2 (Thr202/Tyr204) at dilutions of 1:1000 or 1:500. The secondary antibody was a horseradish peroxidase (HRP)-conjugated goat anti-rabbit IgG (1:2000). All antibodies were from CellSignaling Technology, USA. Immunodetection, imaging and data analysis was performed using SignalFire™ enhanced chemiluminescent (ECL) substrate (CellSignaling Technology, USA), a ChemiDoc™ MP imaging system and Image Lab™ software (Bio-Rad, Germany). Data are presented as phospho-protein/total protein ratios.

Glucose stimulated insulin secretion (GSIS) assay

On day 1 of the experiment, INS-1 cells were detached by Trypsin/EDTA treatment, counted using a CASY TT cell counter (Schärfe, Germany), seeded into 35 mm cell culture dishes (Sarstedt, Austria) at a density of ~400,000 cells per dish, and cultured in RPMI1640 (Sigma Aldrich) supplemented with 1 mM sodium pyruvate (Sigma Aldrich), 23.8 mM sodium bicarbonate (AppliChem), 84.4 µM 2-mercaptoethanol (Sigma Aldrich), 10 mM HEPES (AppliChem) and 5% FBS Superior (Biochrom) at 37°C, 5% CO_2 and 95% air. On day 3, INS-1 cells were gently washed with PBS and then preconditioned for 30 minutes in 2 ml per cell culture dish of glucose-free Krebs Ringer HEPES buffer (KRH 0 Gluc) containing either 0.1% DMSO (KRH 0 Gluc + D; solvent control) or 50 µM of quercetin (KRH 0 Gluc + Q), or rutin (KRH 0 Gluc + R). Preconditioning was followed by the treatment of the cells for one hour with 1 ml per cell culture dish of either KRH 0 Gluc + D, KRH 0 Gluc + Q, KRH 0 Gluc + R, or KRH containing 20 mM glucose (KRH 20 Gluc) and 0.1% DMSO (KRH 20 Gluc + D; solvent control), or 50 µM quercetin (KRH 20 Gluc + Q), or rutin (KRH 20 Gluc + R). Preconditioning and treatment of cells was carried out at 37°C in humidified air. At the end of the treatment period, 200 µl of each cell culture supernatant was collected, centrifuged (800×g, 5 minutes at 4°C) and stored at -20°C. Cells were then detached from each cell culture dish by Trypsin/EDTA treatment and the number of cells per dish determined as described above. The composition of KRH 0 Gluc was (in mM): 145 NaCl, 3.6 KCl, 1.5 $CaCl_2$, 0.5 $MgCl_2$, 10 HEPES, 0.5 NaH_2PO_4, 5 $NaHCO_3$ with 0.1% bovine serum albumin (BSA; fraction V, fatty acid free), pH 7.4 (adjusted with NaOH). KRH 20 Gluc had the same composition as KRH 0 Gluc, except that NaCl was reduced to 132 mM and 20 mM glucose added.

ELISA, insulin release

Insulin concentration in the cell culture supernatants was determined by a rat insulin ELISA (Mercodia, Sweden) according to the protocol suggested by the supplier. The insulin concentration in the cell culture supernatants was normalized to the number of cells (determined at the end of the treatment period (see above)) in each of the corresponding cell culture dishes, and expressed as µg/l per 10^5 cells.

Electrophysiology

INS-1 cells were seeded on poly-D-lysine-coated glass coverslips, cultured under standard conditions and used for patch clamp experiments after 24–48 hrs. The coverslips were transferred to a recording chamber and mounted on an Olympus IMT-2 inverted microscope. All experiments were performed at room temperature in the conventional 'ruptured' patch clamp mode. Patch electrode resistances were 3–5 MΩ. Data were acquired and analyzed using an EPC-10 amplifier and Pulse/FitMaster software (HEKA, Germany). Cell membrane potential recordings were performed in the zero current clamp mode. The intracellular (pipette) solution contained (in mM): 120 potassium *D*-gluconate, 5 NaCl, 10 KCl, 2 $CaCl_2$, 4 $MgCl_2$, 2 ATP (Mg^{2+} salt), 5 HEPES free acid (FA), 10 EGTA, 5 raffinose (pH 7.2 adjusted with KOH, 300 mOsm/kg). The extracellular solution contained (in mM): 140 NaCl, 5.6 KCl, 2.5 $CaCl_2$, 1.5 $MgCl_2$, 10 HEPES FA, 4.5 D-glucose, 5 mannitol (pH 7.4 adjusted with NaOH, 300 mOsm/kg). Whole cell K_{ATP} currents were recorded using same solutions at a holding potential of -70 mV and during 500-ms pulses to -80 and -60 mV at 10-s intervals as previously described [51, 52]. In this range of potentials, the membrane conductance is predominately determined by K_{ATP} currents [53]. The pipette solution for whole cell Ba^{2+} current recordings contained (in mM): 100 CsCl, 5 $MgCl_2$, 2 ATP (Mg^{2+} salt), 10 HEPES FA, 11 EGTA, 65 raffinose (pH 7.2 adjusted with CsOH, 310 mOsm/kg). The extracellular solution consisted of (in mM): 80 tetraethylammonium (TEA)-Cl, 10 $BaCl_2$, 10 HEPES FA, 5 D-glucose, 120 mannitol (pH 7.2 adjusted with TEA-OH, 303 mOsm/kg). Ba^{2+} currents were elicited by voltage ramps from -100 to +100 mV (500 ms duration, 10-s intervals) from a holding potential of -70 mV [52]. Osmolalities were measured with a vapor pressure osmometer (Wescor, USA). A gravity-driven perfusion system (ALA Scientific Instruments, Inc., USA) with a flow-rate of 3–5 ml/min was used for extracellular solution exchange. Drugs were added to the extracellular solutions as indicated.

Calcium imaging

Intracellular Ca^{2+} was monitored by time-lapse fluorescence imaging. Cells grown for 24–48 hrs in glass-bottom petri dishes (3–cm diameter; MatTek Corporation, USA) under standard cell culture conditions were loaded with 2 μM Fura-2/AM plus 0.08% Pluronic F-127 (Molecular Probes–LifeTechnologies) for 20 minutes at 37°C in the dark in serum-free medium. Cells were washed once and incubated for further 20 minutes in the dark to allow for complete de-esterification of the dye. Dishes were placed on the microscope (iMIC; TILL Photonics–FEI, Germany), which was equipped with a filter set consisting of a 395 nm clean-up filter, a 409 nm beamsplitter and a 510/84 nm bandpass filter (AHF Analysentechnik, Germany) compatible with the Polychrome V monochromator (TILL Photonics) used for dye excitation. Cells were alternately illuminated at 340 and 380 nm for 100–200 ms at 10–second intervals. The emitted light was passed through the clean-up filter, the beamsplitter and the bandpass emission filter before detection by a PCO Sensicam QE CCD camera (PCO AG, Germany). Life Acquisition and Offline Analysis Software (TILL Photonics) was used for microscope, camera and monochromator control, data acquisition and analysis. Cells were continuously perfused with a solution containing (in mM): 140 NaCl, 5.6 KCl, 2.5 $CaCl_2$, 1.5 $MgCl_2$, 10 HEPES FA, 4.5 D-glucose, 5 mannitol (pH 7.2 adjusted with NaOH, 296 mOsm/kg) at a flow rate of 2–3 ml/minute. The Ca^{2+}-free extracellular solution was prepared by omission of $CaCl_2$ and addition of 2 mM EGTA. Drugs were added to the solution as indicated in the figure legend (Fig. 6). The image background was recorded from cell free areas and subtracted from the respective signals. Data are given as 340/380 nm excitation ratios detected at 510 nm.

Statistics and data presentation

Data are expressed as mean ± SEM of at least three biological replicates (n≥3). In all experimental series, solvent control samples were included and compared to untreated controls. In neither series a statistically significant difference between untreated- and solvent (DMSO)-treated cells was observed. Statistical analysis was carried out using Student's t-test or one-way ANOVA with Dunnett's, or Bonferroni's post-test, as applicable. Means were considered significantly different at *p*-values <0.05. $^{*/\#}$, **, ***, **** denotes $p < 0.05$, $p < 0.01$, $p < 0.001$ and $p < 0.0001$, respectively. ns = not significant. n refers to the number of independent experiments. Data were analyzed and plotted using GraphPad Prism 6 (GraphPad Software, USA) or Igor Pro 6 (WaveMetrics, Inc., USA).

Results

Using a resazurin-based assay, we found that incubation with rutin, quercetin, or the PI3K inhibitor LY294002 for 48 hrs dose-dependently reduced INS-1 cell viability with IC_{50} values of ~75 μM, ~25 μM and ~3.5 μM, respectively (Fig. 1A). Addition of 10 μM insulin to the culture medium over 48 hrs stimulated cell proliferation, but had no influence on the inhibiting effect of quercetin on cell viability (Fig. 1B). To test if the effects of rutin and quercetin on cell viability were related to induction of apoptosis, we performed Annexin-V binding assays to quantify phosphatidylserine (PS) exposure and measurements of the mean cell volume (MCV) using flow cytometry. Quercetin (50 μM) significantly increased the percentage of Annexin-V binding (Annexin-V+) cells from 16.2 ± 0.9% to 36.9 ± 8.9% within 48 hrs (Fig. 1C and E) and the MCV of Annexin-V+ cells was significantly lower in quercetin-treated samples compared to control cells (1340.0 ± 202.8 fl vs. 1622.0 ± 135.2 fl, respectively; Fig. 1D). Rutin (50 μM) had no effect on the percentage of Annexin-V+ cells or the MCV.

Given the effects of quercetin and rutin on cell viability, we next tested if the compounds interfere with signaling pathways that regulate cell survival and proliferation. Using Western blot we quantified the abundance of phosphorylated Akt (PKB) and extracellular signal-regulated kinase 1 and 2 (Erk1/2, or p44/42) protein in cells incubated for 2 hrs in absence or presence of rutin or quercetin. We found that quercetin (50 μM) caused a significant decrease in basal- and insulin-stimulated Akt(T308) phosphorylation by ~40% and 50%, respectively, without affecting basal-, or stimulated phosphor (P)-Akt(S473) abundance. Further Erk1/2 phosphorylation was significantly increased by ~50% in quercetin-treated

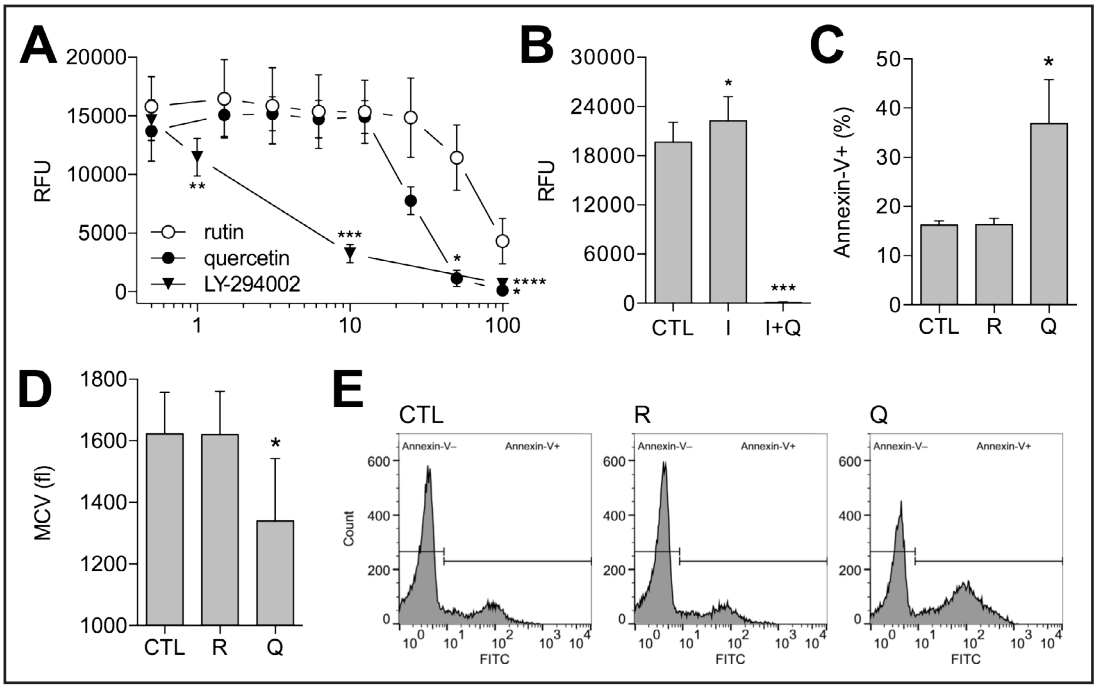

Fig. 1. (A) Dose-dependent inhibition of INS-1 cell viability by rutin (R; n = 4), quercetin (Q; n = 5) and LY294002 (LY; n = 9) measured after 48 hrs. (B) Effects of insulin (10 µM) and insulin (I) plus Q (50 µM) on cell viability within 48 hrs (n = 6). (C) and (D) Phosphatidylserine (PS) exposure (percentage of Annexin-V+ cells) and mean cell volume (MCV), respectively, of INS-1 cells cultured for 48 hrs in absence or presence of R and Q (50 µM each; n = 5) measured by flow cytometry. (E) Data of a single experiment shown as histograms (Annexin-V– and Annexin-V+ cell populations) of cells cultured for 48 hrs in absence or presence of R or Q. Asterisks indicate significant differences to solvent (DMSO) control (CTL); RFU, relative fluorescence units.

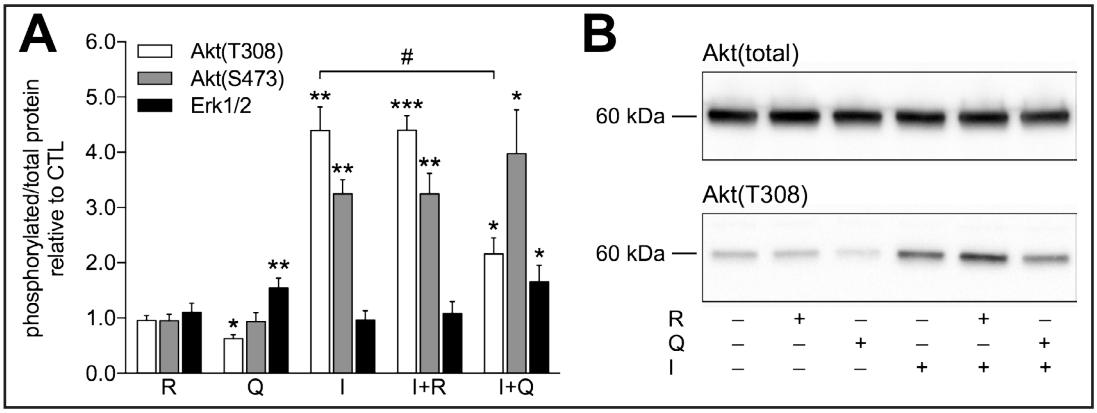

Fig. 2. (A) Western blot analysis of the effect of 50 µM rutin (R) and quercetin (Q) on Akt- and Erk1/2 phosphorylation. Akt(T308) and Erk1/2 (n = 5), Akt(S473) (n = 4). Akt(T308/S473) phosphorylation was stimulated by addition of 10 µM insulin (I) to the culture medium during the 2 hrs incubation period with R and Q. Data are shown as ratios of phosphorylated protein to total protein under the given experimental conditions relative to solvent (DMSO)-treated cells (CTL). Asterisks indicate significant differences to CTL. # indicates a significant difference between I and I+Q for Akt(T308) phosphorylation. (B) Western blot images (cropped) of total Akt protein (upper bands) and Akt(T308)-phosphorylated protein (lower bands) under the indicated experimental conditions.

cells compared to control cells. At the same concentration rutin (50 µM) had no significant effect on (P)-Akt(T308/S473), or P-Erk1/2 protein abundances (Fig. 2).

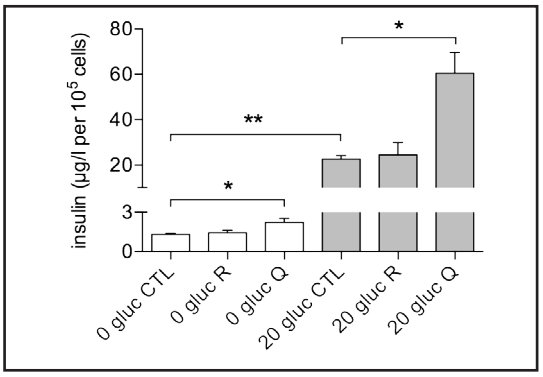

Fig. 3. Effects of quercetin (Q) and rutin (R) on insulin secretion measured by ELISA as cumulative release over 1 h (n = 3). CTL, solvent (DMSO) control. Asterisks indicate significant differences between groups as indicted.

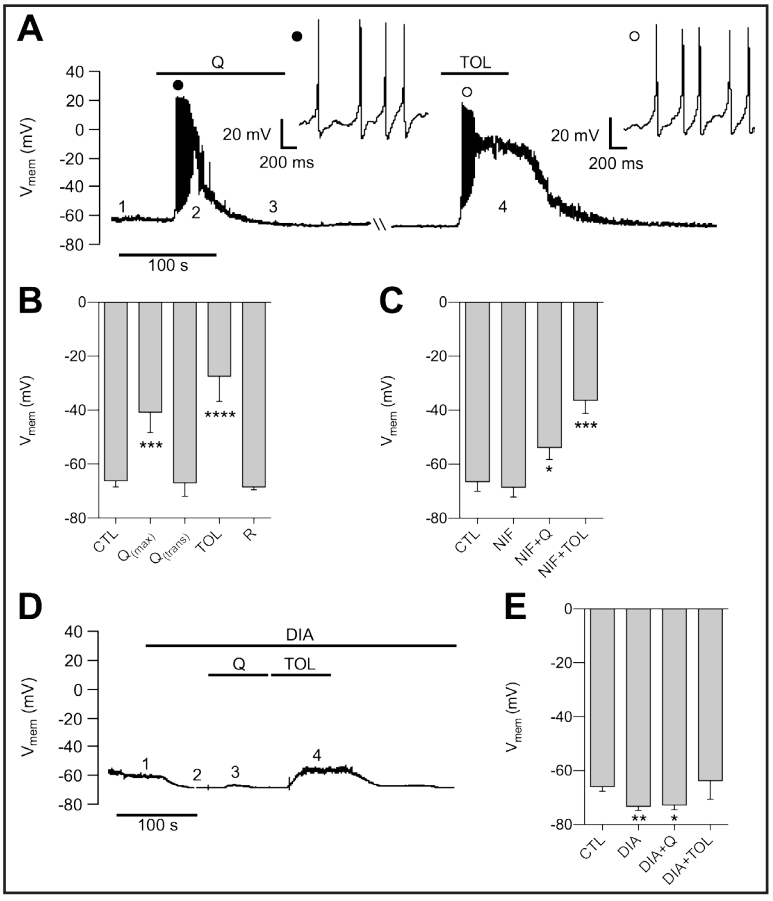

Fig. 4. Effect of quercetin (Q) on the cell membrane potential (V_{mem}) and electrical activity of INS-1 cells. (A) Current clamp recording in absence and presence of Q (50 µM), or tolbutamide (TOL; 50 µM). Sequences of action potentials elicited by Q or TOL are shown as insets at a higher temporal resolution (Q, full symbols; TOL, empty symbols). In contrast to the TOL-induced depolarization, the Q-induced effect is transient with V_{mem} returning to the control level within ~1 min. Numbers 1–4 correspond to those in (B) and indicate time points at which V_{mem} was analyzed. (B) Average V_{mem} under the given conditions. Results of 5–8 individual experiments as shown in (A). $Q_{(max)}$, maximum Q effect; $Q_{(trans)}$, V_{mem} after ~1 min of Q application; TOL, tolbutamide; R, rutin (50 µM). (C) Effects of Q and TOL on V_{mem} in presence of nifedipine (NIF; 10 µM), n = 7–8. (D) Effects of Q and TOL on V_{mem} in presence of diazoxide (DIA; 100 µM). Numbers 1–4 in (D) correspond to those in (E) indicating at which time points V_{mem} was analyzed. (E) Average V_{mem} under the given conditions. Results of 5–8 individual experiments as shown in (D). Asterisks indicate significant differences to solvent (DMSO) control (CTL).

By performing insulin release measurements under basal- and glucose-stimulated conditions using ELISA, we next tested for short-term effects of rutin and quercetin on INS-1 cell function. Basal insulin secretion in glucose-free ringer was 1.3±0.1 µg/l per 100,000 cells (n = 3; Fig. 3). Under 20 mM glucose we observed a 17-fold increase to 22.7 ± 1.6 µg/l per 100,000 cells. Both basal- and glucose-stimulated secretion were significantly augmented 1.7- and 2.7-fold by 50 µM quercetin, respectively, whereas rutin did not significantly affect hormone release.

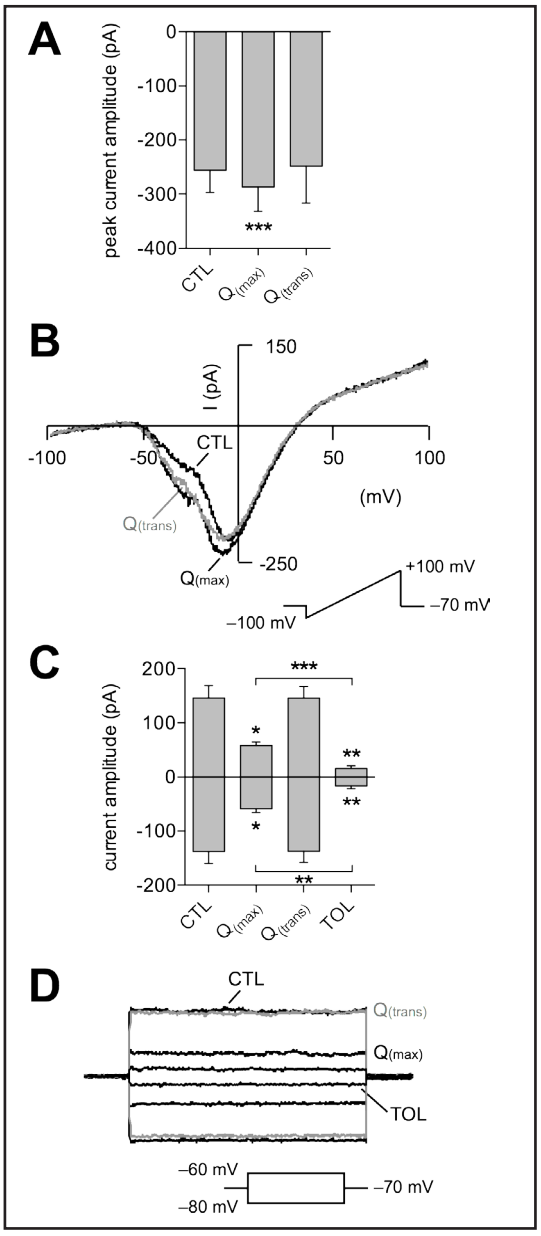

Fig. 5. Effects of quercetin (Q; 50 µM) on whole-cell Ca^{2+} (ICa) and ATP-dependent K^+ currents (IK_{ATP}) in INS-1 cells. (A) Transient increase in peak ICa amplitudes by Q. CTL, solvent (DMSO) control (n = 14); $Q_{(max)}$, maximal effect of Q (n = 14); $Q_{(trans)}$, current amplitudes after ~1 min in continued presence of Q (n = 7). (B) Original ICa tracings of an individual experiment in absence (CTL) and presence of Q. The inset shows the applied voltage-ramp protocol. (C) Inhibition of IK_{ATP} by Q and tolbutamide (TOL) (n = 6). $Q_{(max)}$, maximal effect of Q; $Q_{(trans)}$, current amplitudes after ~1 min in continued presence of Q. (D) Original IK_{ATP} tracings of an individual experiment in absence (CTL) and presence of Q, or TOL. The inset shows the applied voltage-step protocol. Asterisks indicate significant differences to solvent (DMSO) control (CTL), or between groups as indicated.

To test, if stimulated insulin secretion was due to an acute effect of quercetin on the electrophysiological behavior of INS-1 cells, we performed patch clamp recordings of the cell membrane potential (V_{mem}) before and after bath application of quercetin. As shown in Fig. 4A and B, quercetin (50 µM) rapidly depolarized V_{mem} from -65.7 ± 3.7 mV under control conditions to maximally -40.8 ± 7.5 mV (n = 8; Fig. 4B; $Q_{(max)}$), which was associated with action potential firing. In the continued presence of quercetin, the action potential amplitudes gradually decreased and V_{mem} returned to control values within 57.5 ± 5.2 s (Fig. 4B; $Q_{(trans)}$). The ATP-sensitive K^+ current (IK_{ATP}) blocker tolbutamide (50 µM) caused a persistent, reversible depolarization to -27.5 ± 9.3 mV (n = 6). Rutin (50 µM) had no significant effect on V_{mem} (n = 5; p = 0.33). Therefore, we focused on quercetin in the following series of patch clamp experiments and did not further test rutin.

V_{mem} and electrical activity of beta-cells is mainly determined by ATP-sensitive K^+ currents (IK_{ATP}) and voltage-dependent Ca^{2+} conductances (ICa). To find out, if effects on one or both of these conductances (i.e., inhibition of IK_{ATP} and/or activation of ICa) were underlying the quercetin-induced depolarization, we performed additional series of V_{mem} recordings applying the L-type Ca^{2+} current inhibitor nifedipine, or the K_{ATP}-channel opener diazoxide along with quercetin. In the presence of nifedipine (10 µM), which did not significantly affect V_{mem} when applied alone (p = 0.69; n = 8), both quercetin or tolbutamide caused depolarizations from -68.6 ± 3.6 (n = 8) to -53.9 ± 4.4 (n = 8) and -36.3±4.9 mV (n = 7), respectively (Fig. 4C). These changes in V_{mem} were smaller, but not significantly different to the depolarizations induced by quercetin or tolbutamide alone shown in Fig. 4B (p = 0.16 and 0.40, respectively). Application of diazoxide alone (100 µM) caused a significant hyperpolarization of V_{mem} from -65.9 ± 1.8 to -73.3 ± 1.5 mV (n = 8) (Fig. 4D and E). When quercetin was applied in addition of diazoxide, V_{mem} remained hyperpolarized at -72.8 ± 1.7

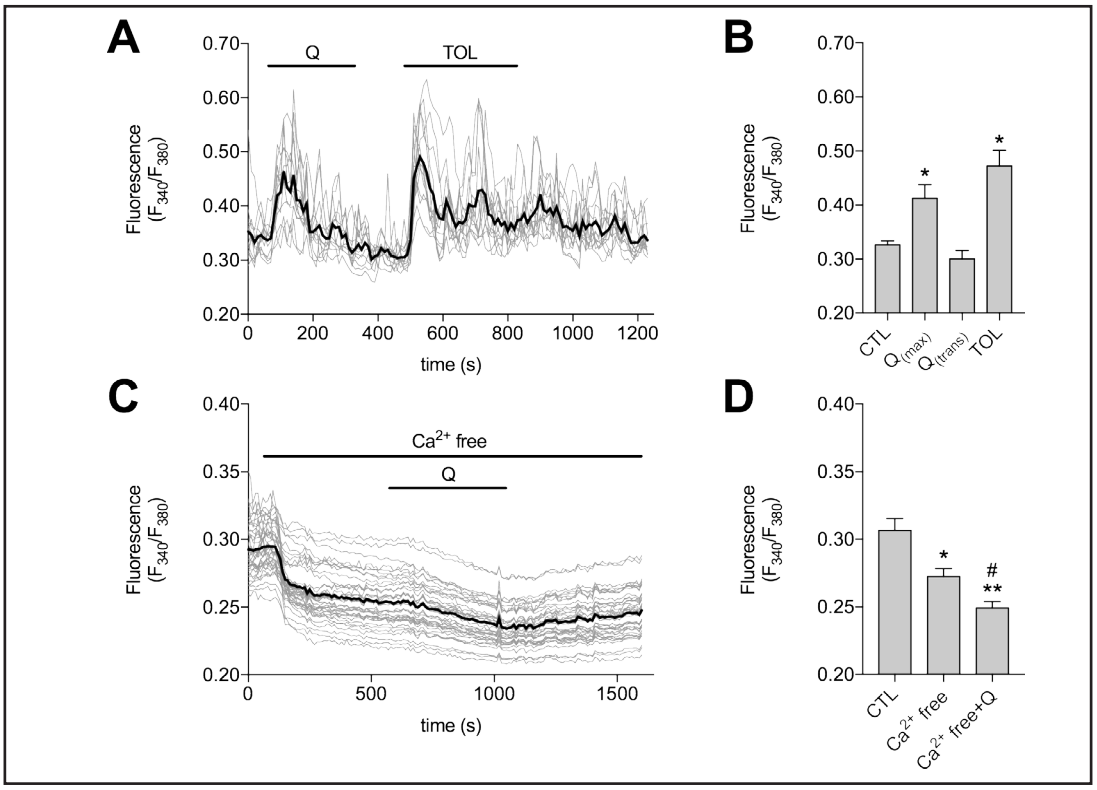

Fig. 6. Quercetin induces a transient elevation in intracellular Ca^{2+} (Ca_i) which requires extracellular Ca^{2+}. Cells were loaded with Fura-2/AM and fluorescence ratios (F_{340}/F_{380}) were recorded in the absence or presence of quercetin (Q; 50 µM) or tolbutamide (TOL; 50 µM). (A) and (C) Responses of single cells (grey tracings) and mean responses (black tracings) of 13 and 39 cells, respectively, of individual experiments. In experiments as shown in (A) Ca^{2+} was present in the extracellular solution during the whole experiment. (B) Bar graph showing the average of the mean responses of 4 individual experiments (13–34 cells per experiment) as shown in (A). $Q_{(max)}$, maximal effect of Q; $Q_{(trans)}$, fluorescence ratios after ~6 min of Q application. (D) Average of mean responses of 4 individual experiments (30–41 cells per experiment) as shown in (C). Ca^{2+} free+Q, fluorescence ratios after ~7 min of Q application in Ca^{2+} free extracellular solution. Asterisks indicate significant differences to solvent (DMSO) control (CTL). # indicates a significant difference to Ca^{2+} free conditions.

mV (n = 8), and also tolbutamide-induced electrical activity and depolarization were largely prevented reaching levels of V_{mem} as measured under control conditions (-63.7 ± 6.9 mV; n = 5; Fig. 4E).

To directly assess possible effects of quercetin on voltage-dependent Ca^{2+} conductances, we measured whole-cell currents in response to voltage ramps from -100 to +100 mV from a holding potential of -70 mV using Ba^{2+} as charge carrier. As characteristic for L-type Ca^{2+} currents, the conductance reached peak amplitudes at high voltage (-5.54 ± 0.86 mV; n = 14) and were sensitive to nifedipine (data not shown). As shown in Fig. 5A and B, quercetin (50 µM) quickly and transiently increased the peak current amplitude from -255.8 ± 41.6 pA (CTL; n = 14) to -286.6±44.9 pA ($Q_{(max)}$; n = 14). In the continued presence of quercetin peak currents then gradually decreased back to control current levels within 66.7 ± 8.0 s ($Q_{(trans)}$; n = 7). While the increase in peak currents by quercetin was transient, a persistent broadening of the current-voltage curve was observed (Fig. 5B).

Given that the ATP-dependent K^+ channel opener diazoxide efficiently prevented quercetin-induced depolarizations, we assumed that apart from ICa stimulation, IK_{ATP} played a major role in mediating the quercetin effect. To test this hypothesis, we measured IK_{ATP} by applying voltage steps to -60 and -80 mV from a holding potential of -70 mV before and after

application of quercetin (50 µM). As shown in Fig. 5C and D, application of quercetin resulted in a maximally ~50% inhibition of IK_{ATP} ($Q_{(max)}$). Like observed for V_{mem} and ICa, this effect showed a rapid onset and then faded over ~1 min (60.00 ± 10.33 s) until control current levels were re-obtained ($Q_{(trans)}$). Current amplitudes at -80 and -60 mV were -137.4 ± 22.8 and 145.8 ± 23.1 pA under control conditions and -58.8 ± 7.2 and 58.1 ± 6.4 pA at $Q_{(max)}$ (n = 6). Tolbutamide at the same concentration (50 µM) caused a significantly stronger and persistent block to -16.6 ± 4.7 and 15.9 ± 4.6 pA (n = 6) at -80 and -60 mV, respectively.

To test if quercetin-induced cell membrane depolarization is reflected in changes in the intracellular Ca^{2+} (Ca_i) concentration, we performed time-lapse Ca^{2+} imaging. In the presence of extracellular Ca^{2+} quercetin (50 µM) elicits a similar rise in Ca_i as 50 µM tolbutamide (Fig. 6A and B). In line with V_{mem} recordings, the effect of quercetin on Ca_i was transient with peak responses after ~1.5 min followed by a decline of the signal in the persisting presence of quercetin. Within ~6 min Ca_i returned to control levels. In the absence of extracellular Ca^{2+} the response to quercetin was completely prevented (Fig. 6C and D). After removal of Ca^{2+}, intracellular Ca^{2+} levels decreased and even dropped further upon application of quercetin.

Discussion

In this study we demonstrate that the acute application of quercetin leads to stimulation of both basal and glucose stimulated insulin secretion (GSIS) in rat insulinoma INS-1 cells (Fig. 3). This is in agreement with previous studies, showing potentiation of GSIS by quercetin in INS-1 cells [19] and INS-1E cells [18]. As underlying mechanisms, we could identify simultaneous transient inhibition of K_{ATP} channels and a transient activation of voltage-gated Ca^{2+} channels. While an effect of quercetin on K_{ATP} channels has not yet been described, activation of ICa has been shown in INS-1 cells and pancreatic islets [17]. In contrast to that study where quercetin only slightly affected V_{mem} and caused a permanent activation of Ca^{2+} channels, we observed a transient depolarization of V_{mem} and Ca^{2+} channel activation. The quercetin effects on V_{mem}, ICa and IK_{ATP} rapidly reached peak values and then gradually diminished to control values within ~1 minute (Fig. 4 and 5). However, the broadening of the Ca^{2+}-current-voltage curve under quercetin, which persists after peak current amplitudes returned to control values (Fig. 5B), might indicate the activation of an additional, nifedipine-insensitive Ca^{2+} current component by quercetin. This might explain that, although nifedipine cannot prevent the quercetin-induced depolarization, the magnitude of the effect is slightly (though not significantly) smaller in the presence of nifedipine compared to the effects in its absence (15 mV *vs.* 25 mV depolarization by quercetin in presence *vs.* absence of nifedipine; Fig. 4B and C). The K_{ATP} channel opener diazoxide (100 µM) caused a significant hyperpolarization and completely prevented quercetin and tolbutamide-induced depolarization of V_{mem} and electrical activity (Fig. 4D and E), suggesting that K_{ATP} channels are a direct target of quercetin. Taken together we conclude that the stimulating effect of the aqueous extract of *Leonurus sibiricus* L. observed in INS-1E cells [1] can be attributed at least in part to its constituent quercetin. In other cell types, quercetin has also been reported to act on Ca^{2+}- and K^+- and channels. It was found to inhibit inward Ca^{2+} currents through L-type voltage-gated Ca^{2+} channels in coronary arterial smooth muscle cells and to enhance voltage-gated K^+ channels leading to vasorelaxation [54]. In coronary artery smooth muscle cells quercetin was shown to promote relaxation by stimulation of large-conductance Ca^{2+}-activated K^+ currents [55]. In cultured murine intestinal cells of Cajal quercetin attenuates pacemaker activity by inhibiting TRPM7 channels and also Ca^{2+}-activated Cl^- channels (TMEM16A, ANO1) *via* opioid receptor signaling pathways [56]. In rat tail artery smooth muscle cells with intact endothelium quercetin leads to relaxation even though it acts as activator of L-type Ca^{2+} channels. In these cells it leads to a reversible increase in amplitude and a shift of the activation curve to more negative potentials while it slows the activation and deactivation kinetics as well as the rate of recovery from inactivation [57, 58]. Rutin had no effect on L-type Ca^{2+} currents [58]. For the first time we show here that quercetin inhibits

inwardly rectifying ATP-sensitive K^+ currents. This might be highly relevant for K_{ATP} channels in other tissues and organs like vascular smooth muscle, skeletal muscle, cardiomyocytes or kidney cells. It needs to be tested in future studies, if this effect of quercetin is specific for the IK_{ATP} of insulin-secreting cells (K_{ir} 6.2), or if other subtypes of inwardly-rectifying K^+ channels are also affected.

Quercetin-induced cell membrane depolarization and electrical activity is reflected by a transient elevation in the intracellular Ca^{2+} (Ca_i) concentration with peak responses similar to those of tolbutamide (Fig. 6). This is in line with the effect of aqueous *Leonurus sibiricus* L. extract we previously observed in INS-1E cells [1], but contrasts the findings of Bardy et al., who described a persistent effect of quercetin on Ca_i in INS-1 cells along with an activation of L-type Ca^{2+} channels [17]. However, in accordance with this study we find that in the absence of extracellular Ca^{2+} quercetin fails to elevate Ca_i, which clearly shows that the rise in Ca_i is due to Ca^{2+} influx and not due to release from intracellular stores. This supports the conclusion that quercetin interferes with stimulus-secretion-coupling [59] by inducing V_{mem} depolarization and electrical activity, which leads to a rise in Ca_i and insulin release.

In a number of studies flavonoids and other polyphenolic compounds have been shown to interfere with cell signaling pathways that regulate cell survival and proliferation by affecting key kinases such as PI3K, Akt (PKB) and extracellular signal-regulated kinase 1 and 2 (Erk1/2, or p44/42) [19, 39-41, 46, 60]. As shown in the present study, rutin, quercetin and the PI3K inhibitor LY294002 cause a dose-dependent reduction in cell viability (Fig. 1). Within 2 hrs, quercetin causes a significant decrease in basal- and insulin-stimulated Akt(T308) phosphorylation without affecting P-Akt(S473) abundance and an increase in Erk1/2 phosphorylation (Fig. 2). The decreased Akt(T308) phosphorylation is therefore most likely due to inhibition of PI3K signaling by quercetin [61]. In a previous study we have shown that Akt phosphorylation is inhibited by resveratrol, another flavonoid, which was accompanied, however, by inhibition of insulin secretion [46]. Erk1/2 activation and stimulated insulin secretion by quercetin has already previously been described in INS-1 cells [19]. However, in this study quercetin had no effect on viability at a concentration of 20 µM where we find viability to be reduced by 50% (Fig. 1). 50 µM quercetin significantly increases the percentage of Annexin-V+ cells compared to control cells within 48 hrs and the MCV of quercetin-treated cells is significantly lower, indicating apoptotic cell shrinkage (apoptotic volume decrease, AVD [62]), while rutin does not exert any effect on Annexin-V binding, Erk1/2 or Akt phosphorylation (Fig. 1 and 2). Hence, quercetin but not rutin induces apoptosis in INS-1 cells. It is important to note that we observed a ~20% increase in Annexin-V+ cells but a ~90% reduction of resorufin fluorescence under 50 µM quercetin, which suggests that the quercetin effect might not only be caused by induction of apoptosis, but mainly by a stop of cell proliferation. The inhibitory effect of quercetin on cell viability contrasts the finding that the *Leonurus sibiricus* L. extracts enhances proliferation in INS-1E cells [1]. We assume that the effects of other constituents in *Leonurus sibiricus* L. extracts overrule the anti-proliferative/pro-apoptotic effects of quercetin and rutin shown here.

The concentrations of quercetin and rutin we tested (1.5–100 µM) are in the range as used in other studies on effects on insulin secretion and the electrophysiological behavior of insulinoma cells [17-19]. A significant increase in Ca_i has been shown at 2 µM quercetin in INS-1 cells as well as in dispersed rat pancreatic islets [17]. Glucose-stimulated insulin release was significantly increased at 1 µM in INS-1E cells [18]. Anti-proliferative, pro-apoptotic effects of quercetin on different cancer cell lines have been shown at concentrations from 10 µM up to 1 mM [39-43] and we show a significantly reduced cell viability and increased percentage of Annexin-V+ cells at 50 µM. Such concentrations are unlikely to be achieved *in vivo* upon oral or intravenous administration of the compound. In *in vivo* studies by Egert et al., in which quercetin has been shown to significantly reduce systolic blood pressure, oxidized LDL and TNF-α in overweight patients with high cardiovascular disease risk, mean fasting plasma quercetin concentrations of 269 nmol/l were measured after a daily intake of 150 mg quercetin [13, 31]. Other bioavailability studies report plasma quercetin concentration from 50 nM up to 1.6 µM depending if subjects were consuming habitual diets,

quercetin rich diets or the pure compound [3]. Quercetin is rapidly absorbed in the proximal parts of the gastrointestinal tract, whereas absorption of rutin occurs in the distal parts and is slow, since it must be hydrolyzed by the colonic microflora [3, 4, 63, 64]. Like other flavonoids quercetin almost exclusively appears in the serum as glucuronide and sulfate conjugates, which have been shown to retain their antioxidant properties and which are slowly eliminated (half-lives from 11 to 28 hrs have been reported) so that repeated intake of rutin and quercetin-containing diet might lead to accumulation of metabolites in blood [3, 63-66]. How far these metabolites can affect beta-cell function and viability as shown here needs to be investigated in further studies.

Insulinoma-derived INS-1 and INS-1E cells are reliable beta-cell surrogates displaying electrophysiological properties, secretagogue-induced electropysiological activity, Ca^{2+} signaling, stimulus-secretion-coupling and sulfonylurea and diazoxide-sensitivities similar to native islets [48, 67]. Insulinoma cells have been used in numerous studies on drugs interfering with signal transduction pathways involved in regulating beta-cell mass, proliferation and apoptosis [19, 44-47, 49]. However, altered secretory responses and cell signaling processes regulating proliferation and apoptosis compared to native beta-cells must be considered. For instance differences among beta-cell lines and pancreatic islets in their insulin release responses to osmotic stimuli have been shown [68, 69]. Therefore, future studies on native beta-cells need to be performed to validate the significance of our findings. Especially it needs to be clarified if the effect of quercetin on cell viability is specific for insulinoma cells or also have implications for native beta-cells.

We conclude that in INS-1 cells quercetin acutely stimulates insulin release, presumably by transient K_{ATP} channel inhibition and simultaneous transient stimulation of voltage-sensitive Ca^{2+} channels. Long-term application of quercetin and rutin for 48 hrs, however, inhibits cell proliferation and quercetin induces apoptosis, most likely by inhibition of PI3K/Akt signaling. Our data contribute to a better understanding of the mechanism of action of quercetin on beta-cell function and viability.

Acknowledgements

We thank Prof. Claes B. Wolheim for providing the INS-1 cells. We thank Leman Emin and Katharina Schuhbeck for their assistance. This project was supported by the PMU grants R-09/04/009-JAK and R-11/02/024-JAK to MJ.

Disclosure Statement

The authors declare that there are no conflicts of interest.

References

1 Schmidt S, Jakab M, Jav S, Streif D, Pitschmann A, Zehl M, Purevsuren S, Glasl S, Ritter M: Extracts from Leonurus sibiricus L. increase insulin secretion and proliferation of rat INS-1E insulinoma cells. J Ethnopharmacol 2013;150:85-94.

2 Pitschmann A, Zehl M, Heiss E, Purevsuren S, Urban E, Dirsch VM, Glasl S: Quantitation of phenylpropanoids and iridoids in insulin-sensitising extracts of Leonurus sibiricus L. (Lamiaceae). Phytochem Anal DOI:10.1002/pca.2583.

3 Erlund I: Review of the flavonoids quercetin, hesperetin, and naringenin. Dietary sources, bioactivities, bioavailability, and epidemiology. Nutr Res 2004;24:851-874.

4 Shin NR, Moon JS, Shin SY, Li L, Lee YB, Kim TJ, Han NS: Isolation and characterization of human intestinal Enterococcus avium EFEL009 converting rutin to quercetin. Lett Appl Microbiol 2016;62:68-74.

5 Shen SC, Lee WR, Lin HY, Huang HC, Ko CH, Yang LL, Chen YC: *In vitro* and *in vivo* inhibitory activities of rutin, wogonin, and quercetin on lipopolysaccharide-induced nitric oxide and prostaglandin E2 production. Eur J Pharmacol 2002;446:187-194.

6 La Casa C, Villegas I, Alarcon de la Lastra C, Motilva V, Martin Calero MJ: Evidence for protective and antioxidant properties of rutin, a natural flavone, against ethanol induced gastric lesions. J Ethnopharmacol 2000;71:45-53.
7 Sanders RA, Rauscher FM, Watkins JB, 3rd: Effects of quercetin on antioxidant defense in streptozotocin-induced diabetic rats. J Biochem Mol Toxicol 2001;15:143-149.
8 Kamalakkannan N, Prince PS: Antihyperglycaemic and antioxidant effect of rutin, a polyphenolic flavonoid, in streptozotocin-induced diabetic wistar rats. Basic Clin Pharmacol Toxicol 2006;98:97-103.
9 Potapovich AI, Kostyuk VA: Comparative study of antioxidant properties and cytoprotective activity of flavonoids. Biochemistry (Mosc) 2003;68:514-519.
10 Guardia T, Rotelli AE, Juarez AO, Pelzer LE: Anti-inflammatory properties of plant flavonoids. Effects of rutin, quercetin and hesperidin on adjuvant arthritis in rat. Farmaco 2001;56:683-687.
11 Janbaz KH, Saeed SA, Gilani AH: Protective effect of rutin on paracetamol- and CCl4-induced hepatotoxicity in rodents. Fitoterapia 2002;73:557-563.
12 Yang K, Lamprecht SA, Liu Y, Shinozaki H, Fan K, Leung D, Newmark H, Steele VE, Kelloff GJ, Lipkin M: Chemoprevention studies of the flavonoids quercetin and rutin in normal and azoxymethane-treated mouse colon. Carcinogenesis 2000;21:1655-1660.
13 Egert S, Bosy-Westphal A, Seiberl J, Kurbitz C, Settler U, Plachta-Danielzik S, Wagner AE, Frank J, Schrezenmeir J, Rimbach G, Wolffram S, Muller MJ: Quercetin reduces systolic blood pressure and plasma oxidised low-density lipoprotein concentrations in overweight subjects with a high-cardiovascular disease risk phenotype: a double-blinded, placebo-controlled cross-over study. Br J Nutr 2009;102:1065-1074.
14 Kim E-K, Kwon K-B, Song M-Y, Han M-J, Lee J-H, Lee Y-R, Lee J-H, Ryu D-G, Park B-H, Park J-W: Flavonoids Protect Against Cytokine-Induced Pancreatic β-Cell Damage Through Suppression of Nuclear Factor κB Activation. Pancreas 2007;35:e1-e9.
15 Martinez-Florez S, Gutierrez-Fernandez B, Sanchez-Campos S, Gonzalez-Gallego J, Tunon MJ: Quercetin attenuates nuclear factor-κB activation and nitric oxide production in interleukin-1β-activated rat hepatocytes. J Nutr 2005;135:1359-1365.
16 Ruiz PA, Braune A, Holzlwimmer G, Quintanilla-Fend L, Haller D: Quercetin inhibits TNF-induced NF-κB transcription factor recruitment to proinflammatory gene promoters in murine intestinal epithelial cells. J Nutr 2007;137:1208-1215.
17 Bardy G, Virsolvy A, Quignard JF, Ravier MA, Bertrand G, Dalle S, Cros G, Magous R, Richard S, Oiry C: Quercetin induces insulin secretion by direct activation of L-type calcium channels in pancreatic beta cells. Br J Pharmacol 2013;169:1102-1113.
18 Bhattacharya S, Oksbjerg N, Young JF, Jeppesen PB: Caffeic acid, naringenin and quercetin enhance glucose-stimulated insulin secretion and glucose sensitivity in INS-1E cells. Diabetes Obes Metab 2014;16:602-612.
19 Youl E, Bardy G, Magous R, Cros G, Sejalon F, Virsolvy A, Richard S, Quignard JF, Gross R, Petit P, Bataille D, Oiry C: Quercetin potentiates insulin secretion and protects INS-1 pancreatic beta-cells against oxidative damage via the ERK1/2 pathway. Br J Pharmacol 2010;161:799-814.
20 Kappel VD, Frederico MJ, Postal BG, Mendes CP, Cazarolli LH, Silva FR: The role of calcium in intracellular pathways of rutin in rat pancreatic islets: potential insulin secretagogue effect. Eur J Pharmacol 2013;702:264-268.
21 Cherniack EP: Polyphenols: planting the seeds of treatment for the metabolic syndrome. Nutrition 2011;27:617-623.
22 Anhe GF, Okamoto MM, Kinote A, Sollon C, Lellis-Santos C, Anhe FF, Lima GA, Hirabara SM, Velloso LA, Bordin S, Machado UF: Quercetin decreases inflammatory response and increases insulin action in skeletal muscle of ob/ob mice and in L6 myotubes. Eur J Pharmacol 2012;689:285-293.
23 Rivera L, Moron R, Sanchez M, Zarzuelo A, Galisteo M: Quercetin ameliorates metabolic syndrome and improves the inflammatory status in obese Zucker rats. Obesity (Silver Spring) 2008;16:2081-2087.
24 Kobori M, Masumoto S, Akimoto Y, Oike H: Chronic dietary intake of quercetin alleviates hepatic fat accumulation associated with consumption of a Western-style diet in C57/BL6J mice. Mol Nutr Food Res 2011;55:530-540.
25 Panchal SK, Poudyal H, Brown L: Quercetin ameliorates cardiovascular, hepatic, and metabolic changes in diet-induced metabolic syndrome in rats. J Nutr 2012;142:1026-1032.
26 Coskun O, Kanter M, Korkmaz A, Oter S: Quercetin, a flavonoid antioxidant, prevents and protects streptozotocin-induced oxidative stress and β-cell damage in rat pancreas. Pharmacol Res 2005;51:117-123.

27 Jeong SM, Kang MJ, Choi HN, Kim JH, Kim JI: Quercetin ameliorates hyperglycemia and dyslipidemia and improves antioxidant status in type 2 diabetic db/db mice. Nutr Res Pract 2012;6:201-207.
28 Kim JH, Kang MJ, Choi HN, Jeong SM, Lee YM, Kim JI: Quercetin attenuates fasting and postprandial hyperglycemia in animal models of diabetes mellitus. Nutr Res Pract 2011;5:107-111.
29 Hu QH, Wang C, Li JM, Zhang DM, Kong LD: Allopurinol, rutin, and quercetin attenuate hyperuricemia and renal dysfunction in rats induced by fructose intake: renal organic ion transporter involvement. Am J Physiol Renal Physiol 2009;297:F1080-1091.
30 Li JM, Wang W, Fan CY, Wang MX, Zhang X, Hu QH, Kong LD: Quercetin Preserves β-Cell Mass and Function in Fructose-Induced Hyperinsulinemia through Modulating Pancreatic Akt/FoxO1 Activation. Evid Based Complement Alternat Med 2013;2013:303902.
31 Egert S, Boesch-Saadatmandi C, Wolffram S, Rimbach G, Muller MJ: Serum lipid and blood pressure responses to quercetin vary in overweight patients by apolipoprotein E genotype. J Nutr 2010;140:278-284.
32 Kwon O, Eck P, Chen S, Corpe CP, Lee JH, Kruhlak M, Levine M: Inhibition of the intestinal glucose transporter GLUT2 by flavonoids. FASEB J 2007;21:366-377.
33 Hao HH, Shao ZM, Tang DQ, Lu Q, Chen X, Yin XX, Wu J, Chen H: Preventive effects of rutin on the development of experimental diabetic nephropathy in rats. Life Sci 2012;91:959-967.
34 Kappel VD, Zanatta L, Postal BG, Silva FR: Rutin potentiates calcium uptake via voltage-dependent calcium channel associated with stimulation of glucose uptake in skeletal muscle. Arch Biochem Biophys 2013;532:55-60.
35 Hsu CY, Shih HY, Chia YC, Lee CH, Ashida H, Lai YK, Weng CF: Rutin potentiates insulin receptor kinase to enhance insulin-dependent glucose transporter 4 translocation. Mol Nutr Food Res 2014;58:1168-1176.
36 Guo XD, Zhang DY, Gao XJ, Parry J, Liu K, Liu BL, Wang M: Quercetin and quercetin-3-O-glucuronide are equally effective in ameliorating endothelial insulin resistance through inhibition of reactive oxygen species-associated inflammation. Mol Nutr Food Res 2013;57:1037-1045.
37 Nomura M, Takahashi T, Nagata N, Tsutsumi K, Kobayashi S, Akiba T, Yokogawa K, Moritani S, Miyamoto K: Inhibitory mechanisms of flavonoids on insulin-stimulated glucose uptake in MC3T3-G2/PA6 adipose cells. Biol Pharm Bull 2008;31:1403-1409.
38 Wang F, Yang Y: Quercetin suppresses insulin receptor signaling through inhibition of the insulin ligand-receptor binding and therefore impairs cancer cell proliferation. Biochem Biophys Res Commun 2014;452:1028-1033.
39 Xiang T, Fang Y, Wang SX: Quercetin suppresses HeLa cells by blocking PI3K/Akt pathway. J Huazhong Univ Sci Technolog Med Sci 2014;34:740-744.
40 Yuan Z, Long C, Junming T, Qihuan L, Youshun Z, Chan Z: Quercetin-induced apoptosis of HL-60 cells by reducing PI3K/Akt. Mol Biol Rep 2012;39:7785-7793.
41 Gulati N, Laudet B, Zohrabian VM, Murali R, Jhanwar-Uniyal M: The antiproliferative effect of Quercetin in cancer cells is mediated via inhibition of the PI3K-Akt/PKB pathway. Anticancer Res 2006;26:1177-1181.
42 Cui X, Luo Y, Li C, Li Y, Wang Z: Changes of intracellular Ca^{2+} in quercetin-induced autophagy progression. Acta Biochim Biophys Sin (Shanghai) 2015;47:908-914.
43 Lou G, Liu Y, Wu S, Xue J, Yang F, Fu H, Zheng M, Chen Z: The p53/miR-34a/SIRT1 Positive Feedback Loop in Quercetin-Induced Apoptosis. Cell Physiol Biochem 2015;35:2192-2202.
44 Avram D, Ranta F, Hennige AM, Berchtold S, Hopp S, Haring HU, Lang F, Ullrich S: IGF-1 protects against dexamethasone-induced cell death in insulin secreting INS-1 cells independent of AKT/PKB phosphorylation. Cell Physiol Biochem 2008;21:455-462.
45 Bhattacharjee A, Whitehurst RM, Jr., Zhang M, Wang L, Li M: T-type calcium channels facilitate insulin secretion by enhancing general excitability in the insulin-secreting beta-cell line, INS-1. Endocrinology 1997;138:3735-3740.
46 Bortolotti C, Kunit T, Moder A, Hufnagl C, Schmidt S, Hartl A, Langelueddecke C, Fürst J, Geibel J, Ritter M, Jakab M: The phytostilbene resveratrol induces apoptosis in INS-1E rat insulinoma cells. Cell Physiol Biochem 2009;23:245-254.
47 Langelueddecke C, Jakab M, Ketterl N, Lehner L, Hufnagl C, Schmidt S, Geibel JP, Fuerst J, Ritter M: Effect of the AMP-Kinase Modulators AICAR, Metformin and Compound C on Insulin Secretion of INS-1E Rat Insulinoma Cells under Standard Cell Culture Conditions. Cell Physiol Biochem 2012;29:75-86.

48 Asfari M, Janjic D, Meda P, Li G, Halban PA, Wollheim CB: Establishment of 2-mercaptoethanol-dependent differentiated insulin-secreting cell lines. Endocrinology 1992;130:167-178.
49 Panse M, Gerst F, Kaiser G, Teutsch CA, Dolker R, Wagner R, Haring HU, Ullrich S: Activation of extracellular signal-regulated protein kinases 1 and 2 (ERK1/2) by free fatty acid receptor 1 (FFAR1/GPR40) protects from palmitate-induced beta cell death, but plays no role in insulin secretion. Cell Physiol Biochem 2015;35:1537-1545.
50 Nakayama GR, Caton MC, Nova MP, Parandoosh Z: Assessment of the Alamar Blue assay for cellular growth and viability *in vitro*. J Immunol Methods 1997;204:205-208.
51 Hambrock A, de Oliveira Franz CB, Hiller S, Grenz A, Ackermann S, Schulze DU, Drews G, Osswald H: Resveratrol binds to the sulfonylurea receptor (SUR) and induces apoptosis in a SUR subtype-specific manner. J Biol Chem 2007;282:3347-3356.
52 Jakab M, Lach S, Bacova Z, Langeluddecke C, Strbak V, Schmidt S, Iglseder E, Paulmichl M, Geibel J, Ritter M: Resveratrol Inhibits Electrical Activity and Insulin Release from Insulinoma Cells by Block of Voltage-Gated Ca^{2+} Channels and Swelling-Dependent Cl^- Currents. Cell Physiol Biochem 2008;22:567-578.
53 Drews G, Zempel G, Krippeit-Drews P, Britsch S, Busch GL, Kaba NK, Lang F: Ion channels involved in insulin release are activated by osmotic swelling of pancreatic B-cells. Biochim Biophys Acta 1998;1370:8-16.
54 Hou X, Liu Y, Niu L, Cui L, Zhang M: Enhancement of voltage-gated K^+ channels and depression of voltage-gated Ca^{2+} channels are involved in quercetin-induced vasorelaxation in rat coronary artery. Planta Med 2014;80:465-472.
55 Cogolludo A, Frazziano G, Briones AM, Cobeno L, Moreno L, Lodi F, Salaices M, Tamargo J, Perez-Vizcaino F: The dietary flavonoid quercetin activates BKCa currents in coronary arteries via production of H_2O_2. Role in vasodilatation. Cardiovasc Res 2007;73:424-431.
56 Gim H, Nam JH, Lee S, Shim JH, Kim HJ, Ha KT, Kim BJ: Quercetin Inhibits Pacemaker Potentials via Nitric Oxide/cGMP-Dependent Activation and TRPM7/ANO1 Channels in Cultured Interstitial Cells of Cajal from Mouse Small Intestine. Cell Physiol Biochem 2015;35:2422-2436.
57 Saponara S, Sgaragli G, Fusi F: Quercetin as a novel activator of L-type Ca^{2+} channels in rat tail artery smooth muscle cells. Br J Pharmacol 2002;135:1819-1827.
58 Fusi F, Saponara S, Pessina F, Gorelli B, Sgaragli G: Effects of quercetin and rutin on vascular preparations: a comparison between mechanical and electrophysiological phenomena. Eur J Nutr 2003;42:10-17.
59 Ashcroft FM, Rorsman P: Electrophysiology of the pancreatic beta-cell. Prog Biophys Mol Biol 1989;54:87-143.
60 Chan A, Dolinsky V, Soltys C, Viollet B, Baksh S, Light P, Dyck J: Resveratrol inhibits cardiac hypertrophy via AMP-activated protein kinase and Akt. J Biol Chem 2008;283:24194-24201.
61 Vlahos CJ, Matter WF, Hui KY, Brown RF: A specific inhibitor of phosphatidylinositol 3-kinase, 2-(4-morpholinyl)-8-phenyl-4H-1-benzopyran-4-one (LY294002). J Biol Chem 1994;269:5241-5248.
62 Okada Y, Shimizu T, Maeno E, Tanabe S, Wang X, Takahashi N: Volume-sensitive chloride channels involved in apoptotic volume decrease and cell death. J Membr Biol 2006;209:21-29.
63 Manach C, Morand C, Demigne C, Texier O, Regerat F, Remesy C: Bioavailability of rutin and quercetin in rats. FEBS Lett 1997;409:12-16.
64 Manach C, Williamson G, Morand C, Scalbert A, Remesy C: Bioavailability and bioefficacy of polyphenols in humans. I. Review of 97 bioavailability studies. Am J Clin Nutr 2005;81:230S-242S.
65 Morand C, Crespy V, Manach C, Besson C, Demigne C, Remesy C: Plasma metabolites of quercetin and their antioxidant properties. Am J Physiol 1998;275:R212-219.
66 Manach C, Morand C, Crespy V, Demigne C, Texier O, Regerat F, Remesy C: Quercetin is recovered in human plasma as conjugated derivatives which retain antioxidant properties. FEBS Lett 1998;426:331-336.
67 Merglen A, Theander S, Rubi B, Chaffard G, Wollheim CB, Maechler P: Glucose sensitivity and metabolism-secretion coupling studied during two-year continuous culture in INS-1E insulinoma cells. Endocrinology 2004;145:667-678.
68 Orecna M, Hafko R, Bacova Z, Podskocova J, Chorvat DJ, Strbak V: Different secretory response of pancreatic islets and insulin secreting cell lines INS-1 and INS-1E to osmotic stimuli. Physiol Res 2008;57:935-945.
69 Orecna M, Hafko R, Toporcerova V, Strbak V, Bacova Z: Cell swelling-induced insulin secretion from INS-1E cells is inhibited by extracellular Ca^{2+} and is tetanus toxin resistant. Cell Physiol Biochem 2010;26:197-208.